Variational method for liquids moving on a substrate

Xianmin Xu* and Yana Di†

LSEC,Institute of Computational Mathematics and Scientific/Engineering Computing, NCMIS, AMSS, Chinese Academy of Sciences, Beijing 100190, China

Masao Doi‡

Center of Soft Matter Physics and its Applications, Beihang University, Beijing 100191, China.

Abstract

A new variational method is proposed to calculate the evolution of liquid film and liquid droplet moving on a solid substrate. A simple time evolution equation is obtained for the contact angle of a liquid film that starts to move on a horizontal substrate. The equation indicates the dynamical transition at the receding side, and the ridge formation at the advancing side. The same method is applied for the evolution of a droplet that starts to move on an inclined solid surface, and again the characteristic shape change of the droplet is obtained by solving a simple ordinary differential system. We will show that this method has a potential application to a wide class of problems of droplets moving on a substrate.

* xmxu@lsec.cc.ac.cn

† yndi@lsec.cc.ac.cn

‡ Corresponding author. masao.doi@buaa.edu.cn

I. INTRODUCTION

Motion of a liquid droplet on a solid substrate is a phenomenon we see in our everyday life. It is also important in many industrial processes such as coating, painting and printing. Extensive hydrodynamic study of the phenomena has been conducted both theoretically and experimentally[1–5].

Dussan and coworkers[6–8] analysed the droplet shape in a static or quasi-static state and the onset of the droplet movement under gravity or external shear flows. Amar *et al*[9] studied the dynamics of a droplet spreading on a substrate. Extensive works have been done by Limat and his collaborators[10–12] for the droplet sliding down on an inclined substrate. Such studies have clarified characteristic features of sliding droplets, how the sliding velocity depends on inclination angle and droplet volume, how the droplet shape changes with the sliding velocity, and how rivulets appear at the tail of the droplet etc.

Theoretical analysis for the sliding droplet is not easy since one has to deal with the contact line problem. The problem is already quite difficult for the simple two dimensional case[13]. Indeed it has been shown[14] that the conventional boundary conditions (non-slip condition at the solid-liquid interface and the stress condition at the free surface) give a non-physical solution, and certain modifications are needed for the basic equations. Extension of such analysis to the three dimensional case has been done only in limited cases (e.g. [10–12]).

The droplet motion on a sustrate is also a challenging problem from a view point of computational hydrodynamics[15]. Solving the two-phase incompressible Navier-Stokes equation with moving contact angle conditions require high level of numerical techniques and huge computational resources[16]. For a three-dimensional problem, a parallel computation is usually needed to compute the problem accurately. An alternative simplified model has been proposed by Schwartz *et al* [17]. Though the computational cost of this method is less than solving the original Navier-Stokes equation, solving their equation is still not so easy since it is a fourth order nonlinear partial differential equation.

All above methods are based on some partial differential equations(PDEs), where efforts have been focused on how to solve, analytically or numerically, the PDE for given boundary conditions. In this paper, we shall propose an alternative approach. It is not rigorous, but much simpler than the previous methods, and can be applied to a wide class of problems. The method is based on a variational principle called Onsager principle [18, 19], which, in

the present context, is derived from the minimum energy dissipation principle in Stokesian hydrodynamics.

The essence of the method is explained in the next section. Briefly, it is based on the fact that the time evolution of droplet shape is determined by a variational principle, i.e., by minimizing certain function (or functional) of droplet shape change. If we conduct the minimization in the entire parameter space (or functional space), we get the same set of equations used in the conventional theories. Here we conduct the minimization in a restricted functional space, and obtain an approximate evolution equations for the droplet shape.

We believe that such usage of variational principle is new. The novelty rests on the fact that it is a variational principle determining dynamics. In the Stokesian hydrodynamics, it is well known that the fluid velocity is obtained by minimizing the energy dissipation in the system. This principle, known as minimum energy dissipation principle, is a principle which determines the velocity field for given boundary conditions. The variational principle used here is a principle which determines the evolution of the shape of boundaries, and is an extended form of the minimum energy dissipation principle.

Such extended form of the variational principle may not be entirely new. The generalization from the minimum energy dissipation principle to the present variational principle is quite simple, and may have been stated in other context. The variational principle in the present form it has been proposed and used to calculate the shape change of a droplet in an extensional flow[20]. However usage of this principle to problems which involve contact line motion is new, as far as we know. The variational principle is particularly useful here since solving the Stokes equation encounters the difficulty of singularity of solutions [14]. With the present method, one can avoid this difficulty and use it to many other problems in wetting, coating, drying etc.

In this paper, we shall first study a 2D problem of liquid film sliding on a substrate. Though this is a problem that has been studied extensively, we study it again to demonstrate the simplicity of our method. We then apply the method to 3D problem of liquid droplet sliding down on an inclined substrate. We derive a set of non-linear equations for the parameters characterizing the droplet profile, and demonstrate that the present method can predict the evolution of the droplet shape quantitatively.

II. THE VARIATIONAL PRINCIPLE

The variational principle we shall use in this paper can be stated as follows[18, 19]. Consider a Stokesian hydrodynamic system which includes many boundaries (boundary between fluid and solid or fluid and fluid). If the boundaries are moving driven by certain potential forces (gravity, surface tension, etc), the evolution of the system is determined by the following principle: Let $a(t) = \{a_1(t), a_2(t), ...a_N(t)\}$ be the set of the parameters which specify the position of the boundaries. The time evolution of the system, i.e., the time derivative $\dot{a}(t) = \{\dot{a}_1(t), \dot{a}_2(t), ...\dot{a}_N(t)\}$ is determined by the minimum condition for the following function of $\dot{a}$

$$R(\dot{a}, a) = \Phi(\dot{a}, a) + \sum_i \frac{\partial A}{\partial a_i}\dot{a}_i \tag{1}$$

where $A(a)$ is the potential energy of the system, and $\Phi(\dot{a}, a)$ is the energy dissipation function which is defined as the half of the minimum of the energy dissipated per unit time in the fluid when the boundary is changing at rate $\dot{a}$. Since the fluid obeys Stokesian dynamics, $\Phi(\dot{a}, a)$ is always written as a quadratic function of $\dot{a}$.

$$\Phi(\dot{a}, a) = \frac{1}{2}\sum_{i,j} \zeta_{ij}(a)\dot{a}_i\dot{a}_j \tag{2}$$

The minimum condition of eq.(1)

$$\frac{\partial \Phi}{\partial \dot{a}_i} + \frac{\partial A}{\partial a_i} = 0 \quad \text{or} \quad \sum_j \zeta_{ij}(a)\dot{a}_j = -\frac{\partial A}{\partial a_i} \tag{3}$$

represents the force balance of two kinds of forces, the hydrodynamic frictional force $\partial\Phi/\partial\dot{a}_i$, and the potential force $-\partial A/\partial a_i$ in the generalized coordinate.

The above variational principle can be proven directly from the basic equations of Stokesian hydrodynamics [19]. It can also be regarded as a special form of Onsager principle which describes the time evolution of non-equilibrium system characterized by certain set of slow variables[19].

If we use the variational principle to obtain the evolution of the droplet shape in the entire parameter space, we obtain the same set of equations that have been used in previous theories[19]. (Notice that the parameter set $a_i(t)$ can represent a continuous function such as $a(x, t)$, and the function $R(\dot{a}, a)$ may be a functional such as $R[\dot{a}(x, t), a(x, t)]$.) Here we use the variational principle in a restricted parameter space. This gives us a new way of

solving the problems. Application of the Onsager principle to other problems in the same spirit can be found in ref [21–23].

III. LIQUID FILM SLINDING ON A SUBSTRATE

A. Problem

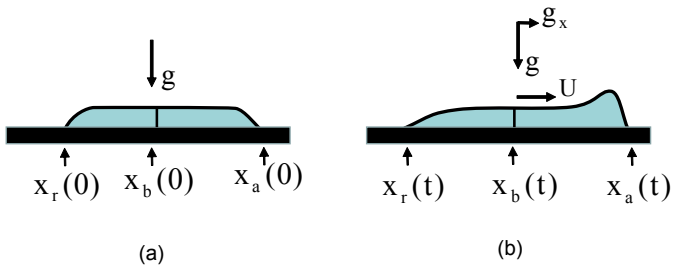

FIG. 1. A liquid film on a horizontal substrate. (a) at equilibrium, and (b) moving under the horizontal acceleration g_x.

To illustrate the essence of the present method, we consider the problem shown in Fig.1. Consider a thin liquid film placed on a horizontal substrate. If the liquid is in equilibrium under gravity(See Fig.1 (a)), the thickness of the liquid is given by $h_e = \theta_e/\kappa_e$, where θ_e is the equilibrium contact angle, and κ_e is the inverse of the capillary length ($\kappa_e = (\rho g/\gamma)^{1/2}$) , where γ and ρ are surface tension and density of the liquid, and g is the gravity constant.

Now suppose that a horizontal acceleration g_x is applied to the liquid in x direction (see Fig.1 (b)). Then the bulk of the liquid starts to move with the velocity

$$U = \frac{\rho g_x h_e^2}{3\eta} \tag{4}$$

where η is the viscosity of the fluid. Here we are assuming that the film is large enough so that the dissipation near the contact points does not affact the velocity in the bulk. Our objective here is to study the evolution of the film shape when it starts to move.

If the span of the film is large, the motion of the advancing side of the film and that of the receding side are independent of each other. Therefore we first discuss the shape change at the receding side.

B. Evolution equation for liquid profile

First, we derive the evolution equation used in the conventional theory from the variational principle. To simplify the calculation, we consider the case that the contact angle is small, and use the lubrication approximation. Let $h(x,t)$ be the thickness of the liquid film at point x and time t, and $v(x,t)$ be the depth-averaged velocity. In the lubrication approximation, the energy dissipation function Φ is written as

$$\Phi[v(x,t);h(x,t)] = \frac{1}{2}\int_{x_r(t)}^{x_b(t)} dx \frac{3\eta}{h(x,t)} v(x,t)^2 \tag{5}$$

where $x_r(t)$ is the position of the contact line, and $x_b(t)$ is the position of a fluid point which can be taken at any point far from the contact line. Since the bulk fluid is moving at speeed U, $x_b(t) = x_b(0) + Ut$.

The fluid velocity $v(x,t)$ is uniquely determined by the time derivative of the liquid profile $\dot{h}(x,t) = \partial h/\partial t$ due to the volume conservation condition for the fluid

$$\dot{h} = -\frac{\partial h(x,t)v(x,t)}{\partial x} \tag{6}$$

or in a integral form

$$h(x,t)v(x,t) = -\frac{d}{dt}\int_{x_r(t)}^{x} dx' h(x',t) \tag{7}$$

The potential energy of the system can be written as a functional of $h(x,t)$:

$$A[h(x,t)] = \int_{x_r}^{x_b} dx \left[\frac{1}{2}\gamma\theta_e^2 + \frac{1}{2}\gamma h'^2 + \frac{1}{2}\rho g h^2 - \rho g_x x h\right] \tag{8}$$

It is easy to show that the minimization of $R = \Phi + \dot{A}$ with respect to v gives the following time evolution equation for $h(x,t)$

$$\frac{\partial h}{\partial t} = -\frac{\gamma}{3\eta}\frac{\partial}{\partial x} h^3 \left[\frac{\partial^3 h}{\partial x^3} + \kappa_e^2\left(\frac{\partial h}{\partial x} - \frac{g_x}{g}\right)\right] \tag{9}$$

Equation (9) is exact within the lubrication approximation, and is essentially the same as that used in the analysis of moving contact line.

C. Approximate calculation

Equation (9) has been obtained by seeking the minimum of R in the entire functional space for $h(x,t)$. Here we seek the minimum of R in a restricted functional space. We

assume that $h(x,t)$ is given by

$$h(x,t) = h_e \left[1 - e^{-\kappa(t)(x - x_r(t))}\right] \tag{10}$$

This functional form is chosen by the following consideration. The function $h(x,t)$ must vanish at the contact point ($x = x_r(t)$) and must approach to h_e in the bulk ($x \to \infty$). Also, the function $h(x,t)$ in the equilibrium state is given given by (10) with $\kappa = \kappa_e = h_e\theta_e$ [3]. Therefore (10) is correct at $t = 0$. When the liquid starts to move at constant velocity U for $t > 0$, the receding contact angle decreases in time. Eq.(10) represents such shape change. (It is known that, in the steady state, the function $h(x,t)$ will have a singular form of $h(x) \propto x(-logx)^{1/3}$[10, 24] in an intermediate rage of x. Here we ignore such complexity and use (10) as a candidate of the approximate profile.)

To determine $\kappa(t)$, we will use the variational principle. If the functional form for $h(x,t)$ is assumed as in eq.(10), the fluid velocity $v(x,t)$ is expressed in terms of $\dot{x}_r$ and $\dot{\kappa}$. Subxtituting eq.(10) into eq.(7), we have

$$v(x,t) = \dot{x}_r - \frac{\dot{\kappa}}{\kappa^2} + \frac{\dot{\kappa}(x - x_r)h_e}{h\kappa} e^{-\kappa(x - x_r)} \tag{11}$$

Since $v(x,t)$ must approach to U for large value of x, we have a relation which constrains $\dot{x}_r$ and $\dot{\kappa}$:

$$U = \dot{x}_r - \frac{\dot{\kappa}}{\kappa^2} \tag{12}$$

Therefore we have only one parameter to be determined, $\kappa(t)$, or the contact angle $\theta(t) = h_e\kappa(t)$.

Using (11) in (5), we have the energy dissipation function Φ expressed as a quadratic function of $\dot{\theta} = h_e\dot{\kappa}$ and U:

$$\Phi = \frac{1}{2}(\zeta_{\theta\theta}\dot{\theta}^2 + 2\zeta_{\theta U}\dot{\theta}U + \zeta_{UU}U^2) \tag{13}$$

Explicit forms of the coefficients $\zeta_{\theta\theta}$, $\zeta_{\theta U}$ are obtained by eqs. (11) and (5). For example, $\zeta_{\theta\theta}$ is given by

$$\zeta_{\theta\theta} = 3\eta \int_{x_r}^{x_b} dx \frac{(x - x_r)^2}{\kappa^2 h^3} x e^{-2\kappa(x - x_r)} \tag{14}$$

The integral shows logarithmic divergence at $x = x_r$, which is characteristic in the contact line dynamics. If we retain only the diverging term, we have

$$\zeta_{\theta\theta} = \frac{3\eta h_e^2}{\theta^5} \log(1/\kappa\epsilon) = \frac{3\ell\eta h_e^2}{\theta^5} \tag{15}$$

where ϵ is the cut off length (of the molecular scale), and ℓ is a a large dimensionless parameter given by $\ell = \log(1/\kappa\epsilon)$, which typically takes the value between 15 to 20 [3]. ℓ depends on κ weakly, but we regard it constant in the following calculation. Similarly, $\zeta_{\theta U}$ is calculated as

$$\zeta_{\theta U} = 3\eta \int_{x_r}^{x_b} dx \frac{1}{\kappa h^2}(x - x_r)e^{-\kappa(x-x_r)} = \frac{3\ell\eta h_e}{\theta^3} \tag{16}$$

By use of (10), this can be written as a function of θ, x_b and x_r. Then the generalized potential force conjugate to θ is calculated by $\partial A/\partial\theta$. Straight forward calculation gives the following result:

$$\begin{aligned}\frac{\partial A}{\partial \theta} &= \frac{\gamma}{\kappa_e}\left[\frac{\theta_e}{4}\left(1 - \frac{\theta_e^2}{\theta^2}\right) + \frac{g_x}{g}\frac{\theta_e^3}{\theta^3}\right] \\ &= \frac{\gamma}{\kappa_e}\left[\frac{\theta_e}{4}\left(1 - \frac{\theta_e^2}{\theta^2}\right) + 3\frac{U}{U^*}\frac{\theta_e}{\theta^3}\right]\end{aligned} \tag{17}$$

where U^* is the velocity defined by $U^* = \gamma/\eta$, and we have used eq.(4) to eliminate g_x.

The variational principle indicates that $\dot{\theta}$ is determined by $\partial\Phi/\partial\dot{\theta} + \partial A/\partial\theta = 0$. Using eqs. (13), (15) (16)and (17), we have the following time evolution equation for the receding contact angle θ.

$$\frac{d\theta}{dt} = -\frac{(\ell+1)\kappa_e\theta^2}{\ell\theta_e}\left[U - \frac{U^*}{12(\ell+1)}\theta(\theta_e^2 - \theta^2)\right] \tag{18}$$

Equation (18) indicates that if the system is at equilibrium at $t = 0$, θ decreases with time and approaches to a constant value θ_r determined by the solution of the following equation

$$U = \frac{U^*}{12(\ell+1)}\theta_r(\theta_e^2 - \theta_r^2) \tag{19}$$

Since the right hand side of eq.(19) has a maximum as a function of θ_r, such steady state is realized only when U is less than this maximum value U_c, which is given by $U_c = U^*\theta_e^3/18\sqrt{3}(\ell+1)$. If U is larger than U_c, the contact angle keeps decreasing and there is no steady state at the receding side. Such dynamical transition is known in the contact line dynamics , and eq. (19) agrees with that given in ref. [3] apart from a numerical factor: in ref. [3], the coefficient $12(\ell+1)$ is replaced by 6ℓ. (Notice that the difference may come from the difference in the problem setup: in the present problem, the bulk fluid is driven by the imposed acceleration g_x (which is related to U), while in ref. [3], there is no external driving force: the contact line is moving due to the difference between θ_r and θ_e.)

Examples of the time evolution is shown in Fig. 2. If $U < U_c$, the film profile approaches to a steady state (Fig. 2 (a)), while if $U > U_c$, the contact angle keeps decreasing in time, and there is no steady state. In the numerical experiment, we chose $\ell = 10$.

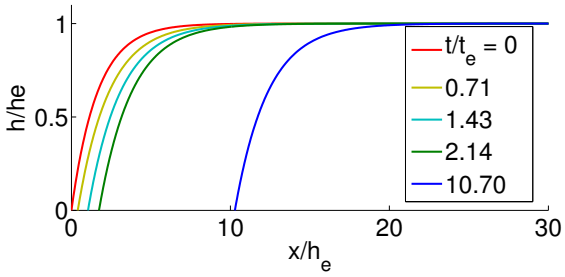

(a)

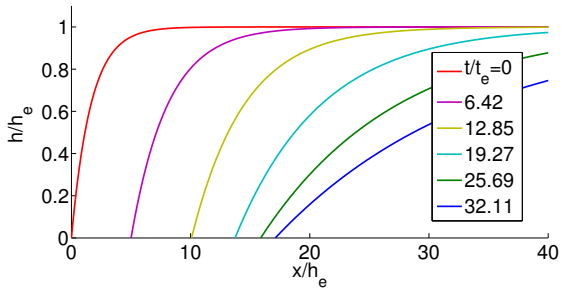

(b)

FIG. 2. The time evolution of the film profile at the receding side, (a) $U = 0.76U_c$. (b) $U = 1.14Uc$, where U_c is the critical velocity at the dynamical transition, and t_e is defined by $t_e = h_e/U$.

The dynamical transition of receding contact line from steady receding state (where the contact line stays at a certain position) to film forming state (where the contact line keeps moving with the substrate) has been extensively studied[25–27], but the nature of the transition is still not settled. De Gennes *et al*[3] showed that the transition is discontinuous, i.e., the steady state contact angle jumps from finite value to zero at a certain critical capillary number. Eggers *et al*[25] argued that the transition is continuous: it occurs at a critical capillary number at which θ_r goes to zero. Experimentally, it is difficult to resolve the issue since the actual transition behavior is much more complex. Snoeijer *et al* [28] showed that transition involves the shape change of the contact line and film profile, and therefore the one-dimensional analysis used in the theoretical studies is not enough to resolve the problem. Maleki *et al* [29] studied the profile of the receding side carefully and concluded that the receding angle may be discontinuous at the transition. Our result is consistent with that of De Gennes *et al*, but the approximate nature of the present analysis is not enough to draw any conclusion on this issue.

Similar analysis can be done for the advancing side. We assume that the film profile is

given by

$$h(x,t) = h_e\left[1 + [a(t)(x_a(t) - x) - 1]e^{-\kappa_e(x_a(t)-x)}\right] \tag{20}$$

where $a(t)$ and $x_a(t)$ are the parameters to be determined. Notice that here we used a different functional form: we assumed that the decay constant in the exponential function is equal to that at equilibrium, κ_e, and that the change of the film shape is represented by the parameter $a(t)$. The contact angle is given by $\theta(t) = [a(t) + \kappa_e]h_e$. Similar calculation as that in the receding side gives the following evolution equation $\theta(t)$

$$\frac{d\theta}{dt} = \frac{\kappa_e}{\ell\theta_e}\Big(U(\ell\theta_e^2 - \theta^2) - \frac{U^*}{6}\theta_e^3\theta(\theta - \theta_e)\Big). \tag{21}$$

Here $\ell = \log(1/(\kappa_e\varepsilon))$.

Fig.3 (a) shows an example of the evolution of the film profile in the advancing side. At the advancing side, steady state is always attained, and a ridge is seen. Fig.3 (b) shows the steady state contact angle as a function of the contact line velocity U. Since the hysteresis effect of the contact line is not considered in the present analysis, the receding contact angle θ_r and the advancing contact angle θ_a are connected smoothly at $U = 0$, i.e, $\theta_r|_{U=0} = \theta_a|_{U=0}$ and $|d\theta_r/dU|_{U=0} = |d\theta_a/dU|_{U=0}$.

D. Calculation with an alternative ansatz

In the previous calculation, we used different forms of function $h(x,t)$ for the advancing and receding sides. It is natural to ask how this assumption affects the results. To answer to this question, we have repeated the calculation by the same functional form for the profile for the two sides.

We assume that for the receding side the profile is given

$$h(x,t) = h_e\big[1 + [a(t)(x - x_r(t)) - 1]e^{-\kappa(t)(x-x_r(t))}\big] \tag{22}$$

and that for the advancing side it is give by

$$h(x,t) = h_e\big[1 + [a(t)(x_a(t) - x) - 1]e^{-\kappa(t)(x_a(t)-x)}\big]. \tag{23}$$

In each side, we have three parameters, a,κ and x_r(or x_a), to be determined. By volume conservation, only two of them are independent. We can choose $a(t)$ and $\kappa(t)$ as variables

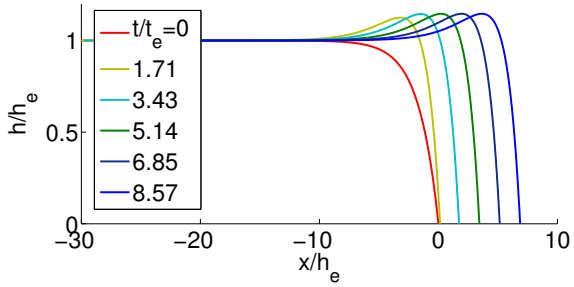

(a)

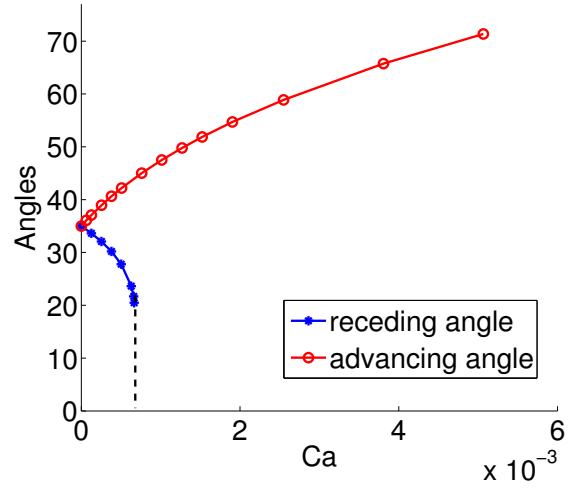

(b)

FIG. 3. (a) The time evolution of the film profile at the advancing side. The bulk velocity is $U = 0.0051U^*$ and $t_e = h_e/U$. (b) Advancing angle and receding angles are plotted against the capillary number $Ca = U/U^*$.

to be determined. By a similar calculation, we derive an ordinary differential equations for a and κ, which are solved numerically.

Fig. 4 shows the changes of $a(t)$ and $\kappa(t)$ in the (a, κ) plane for various initial states where the initial contact angles are taken to be equal to the equilibrium contact angle.

At the receding side (Fig. 4 (a)), it is seen that $a(t)$ decays very quickly to 0, and (22) becomes equivalent to (10). Therefore, at the receding side, the results completely agree with those in the previous calculation. This is seen in the evolution of the profile shown in Fig. 5(a).

On the other hand, at the advancing side, deviations are seen from the previous calculation. In the previous calculation, $\kappa(t)$ was assumed to be equal to the equilibrium value

κ_e, but as it is seen in Fig. 4(b), $\kappa(t)$ decreases in time and approaches to a steady state value(about $0.54\kappa_e$). Accordingly, the liquid profile becomes different from that in the previous calculation (see 5(b)). However, it should be noted that characteristic features of the film shape remain unchanged. Therefore we may conclude that the difference in the film shape between the receding side and the advancing side obtained in the previous calculation is not due to the difference in the ansatz, but due to the difference in physics and that this difference in the physics is correctly captured by the present variational calculation.

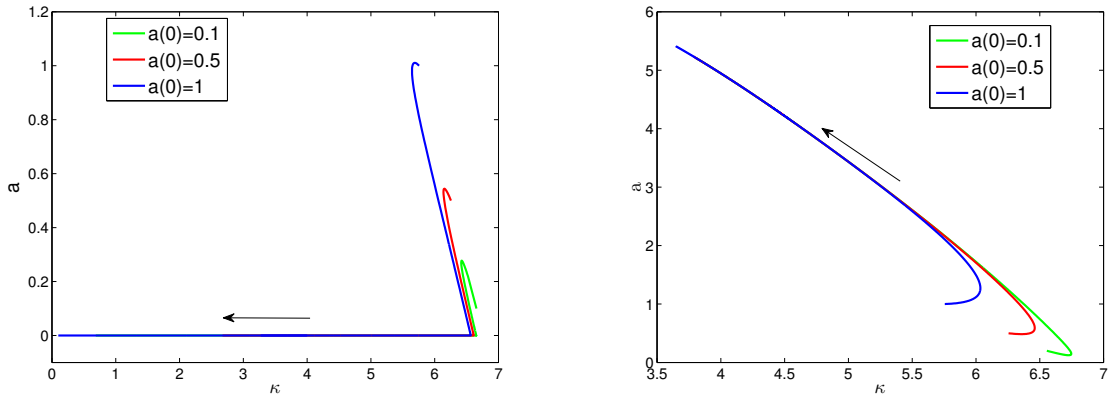

(a) (b)

FIG. 4. (a) phase plane for the receding case; (b) phase plane for the advancing case

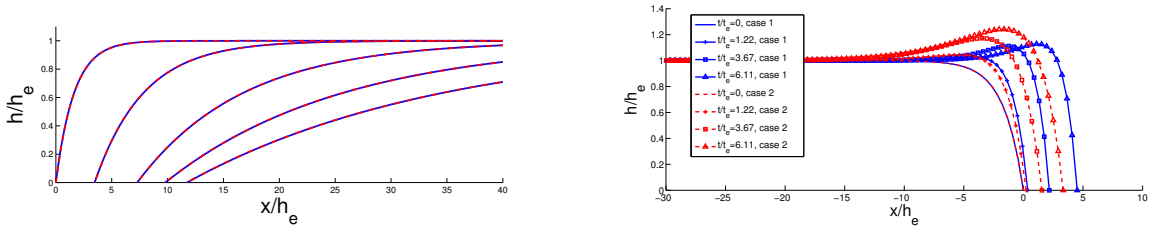

(a) (b)

FIG. 5. (a)Comparison for shape evolution for the receding case at $t/t_e = 0, 6.2129, 15.1346, 24.0563, 32.9780$ (from left to right). Blue: using ansatz (10); Red: using ansatz (22). (b)Comparison for shape evolution for the advancing case. Blue: using ansatz (20); Red: using ansatz (23).

IV. LIQUID DROPLET SLIDING DOWN ON AN INCLINED SUBSTRATE

Next we consider a liquid droplet which was at rest on a horizontal substrate and starts to move when the base substrate is tilted by an angle α against the horizontal plane. We take an orthogonal coordinate; z axis is normal to the substrate, x axis in the downward direction, and y axis is in the horizontal plane. Let $z = h(x, y, t)$ be the function which defines the shape of the droplet at time t.

The shape of a sliding droplets has been studied both experimentally and theoretically[5, 10, 30]. Such studies indicate that the function $h(x, y, t)$ can be approximately represented by

$$h(x, y, t) = H(x, t)\left[1 - \left(\frac{y}{Y(x, t)}\right)^2\right]. \tag{24}$$

where $H(x, t)$ and $Y(x, t)$ are the functions to be determined. According to eq.(24), at a given x coordinate, the droplet thickness decreases parabolically with y and becomes zero at $y = Y(x, t)$. Therefore the contact line of the droplet is given by the function $y = Y(x, t)$. The side view of the droplet is specified by the function $z = H(x, t)$.

To proceed further, we assume that $H(x, t)$ and $Y(x, t)$ have the following form:

$$H(x, t) = (x - a_1(t))(a_2(t) - x)(a_3(t) + a_4(t)x), \tag{25}$$

$$Y(x, t) = (x - a_1(t))^{\frac{1}{2}}(a_2(t) - x)^{\frac{1}{2}}(a_5(t) + a_6(t)x). \tag{26}$$

where $a_i(t)$ $(i = 1, 2, ...6)$ are the parameters which will be be determined by the variational principle. These parameters have the following meaning : a_1 and a_2 represent the x-coordinates of the tail and the front of the contact line. The other parameters a_3, a_4, a_5 and a_6 represent the deformation of the droplet from the equilibrium shape. The fractional power law dependence of $Y(x, t)$ at $x = a_1$ and at $x = a_2$ indicates that the top view of the droplet is round at the front and at the tail, but the tail can have a cusp if $-a_5/a_6$ becomes equal to a_1.

The volume of the droplet Ω is given by

$$\Omega = \int_{a_1}^{a_2} dx \int_{-Y}^{Y} dy h(x, y, t) \tag{27}$$

Since Ω is constant, only five in $a_i(t)$ are independent.

The potential energy of the system is now given by

$$A(a) = \int_{a_1}^{a_2} dx \int_{-Y}^{Y} dy \left[\tfrac{1}{2}\gamma\theta_e^2 + \tfrac{1}{2}\gamma[(\partial_x h)^2 + (\partial_y h)^2] + \tfrac{1}{2}\rho g h^2 \sin\alpha - \rho g x h \cos\alpha\right] \tag{28}$$

This can be expressed as a function of $a = (a_1, a_2, ...a_6)$ with the use of eqs.(24)-(26).

To determine the time evolution of a_i, we need to know the energy dissipation function expressed as a function $\dot{a}_i$. In the lubrication approximation, the energy dissipation in the droplet can be generally written as a functional of velocity fields $v_x(x,y), v_y(x,y)$ as in eq.(5)

$$\Phi[v_x, v_y] = \frac{1}{2}\int_{a_1}^{a_2} dx \int_{-Y}^{Y} dy \frac{3\eta}{h}(v_x^2 + v_y^2) \tag{29}$$

In calculations, a cut-off of the integral is needed and that will generate a *log* term, as in the previous example. In addition, we do not include the dissipation term due to the contact line friction[31, 32], which is small since the size of the droplet considered below is in millimetre scale. If the droplet profile is changing with the rate $\dot{h}$, the velocity field has to satisfy the volume conservation equation

$$\dot{h} = -\partial_x(v_x h) - \partial_y(v_y h) \tag{30}$$

Unlike the previous case, this equation does not determine v_x and v_y uniquely. The variational principle states that the proper energy dissipation function $\Phi(\dot{a})$ are the minimum of $\Phi[v_x, v_y]$ for the velocity field (v_x, v_y) that satisfies the constraint (30).

For eq.(24), eq. (30) is rewritten as

$$\left(1 - \frac{y^2}{Y^2}\right)\left(\dot{H} + \partial_x(v_x H) + H\partial_y v_y\right) + \frac{2Hy}{Y^3}(y\dot{Y} + y v_x \partial_x Y - Y v_y) = 0 \tag{31}$$

This constraint is satisfied if v_x and v_y satisfy

$$\dot{H} + \partial_x(v_x H) + H\partial_y v_y = 0, \tag{32}$$

$$y\dot{Y} + y v_x \partial_x Y - Y v_y = 0. \tag{33}$$

A simple velocity field which satisfy the above equations is

$$v_x(x,y,t) = V(x,t), \quad v_y(x,y,t) = W(x,t)y \tag{34}$$

where $V(x,t)$ and $W(x,t)$ are given by

$$V(x,t) = -\frac{1}{HY}\int_{a_1}^{x}(\dot{H}Y + H\dot{Y})dx, \tag{35}$$

$$W = \frac{1}{Y}\left(\dot{Y} + V\partial_x Y\right). \tag{36}$$

Since $\dot{H}$ and $\dot{Y}$ are expressed as a linear combination of $\dot{a}_i$, eqs.(34),(35) and (36) give the energy dissipation function $\Phi(\dot{a})$ which is a quadratic function of $\dot{a}$.

$$\Phi(\dot{a}) = \frac{1}{2}\sum_{i,j}\zeta_{ij}\dot{a}_i\dot{a}_j \tag{37}$$

where the coefficients ζ_{ij} are functions of $a = (a_1, a_2, ..a_6)$.

Given the free energy $A(a)$ and the energy dissipation function $\Phi(\dot{a})$, the time evolution equation for a_i is obtained as

$$\sum_{j=1}^{6}\zeta_{ij}\dot{a}_j + \frac{\partial A}{\partial a_i} = 0 \tag{38}$$

All quantities in eq.(38) are expressed as function of a_i, and can be evaluated numerically. Equation (38) is then solved numerically.

An example of the results of such calculations is shown in Fig.6-9. Here we consider the system discussed in ref. [33]. A droplet of silicone oil sliding down a glass plate coated with fluoro-polymers. The parameters used in the calculation are $\eta = 104$cP, $\rho = 964\text{kgm}^{-3}$, $\gamma = 20.9\text{mNm}^{-1}$ and $\theta_e = 53^{\text{o}}$(the advancing angle in [33]). The volume of the droplet is 6.3mm^3.

Fig. 6 shows time evolutions of droplets when they starts to slide down on an inclined substrate. Here the droplet is assumed to be at equilibrium on a horizontal substrate at time 0, and then start to slide down when the substrate is inclined at an angle α for $t > 0$. When the inclination angle α is small, the droplet takes a steady state in oval shape with larger curvature at the receding side than at the advancing side (Fig.6 (b),(d)). When the inclination angle α exceeds a certain critical value, a cusp appears gradually at the receding side and the droplet keeps elongated as time goes on (Fig.6 (f))). This corresponds to the experimental observation that the tail of the droplet becomes unstable, and the cusp breaks up, leaving small droplets behind. The inclination angle at which the cusp appears in our simulation is about 30^{o}, while it is about 34^{o} experimentally[5, 33].

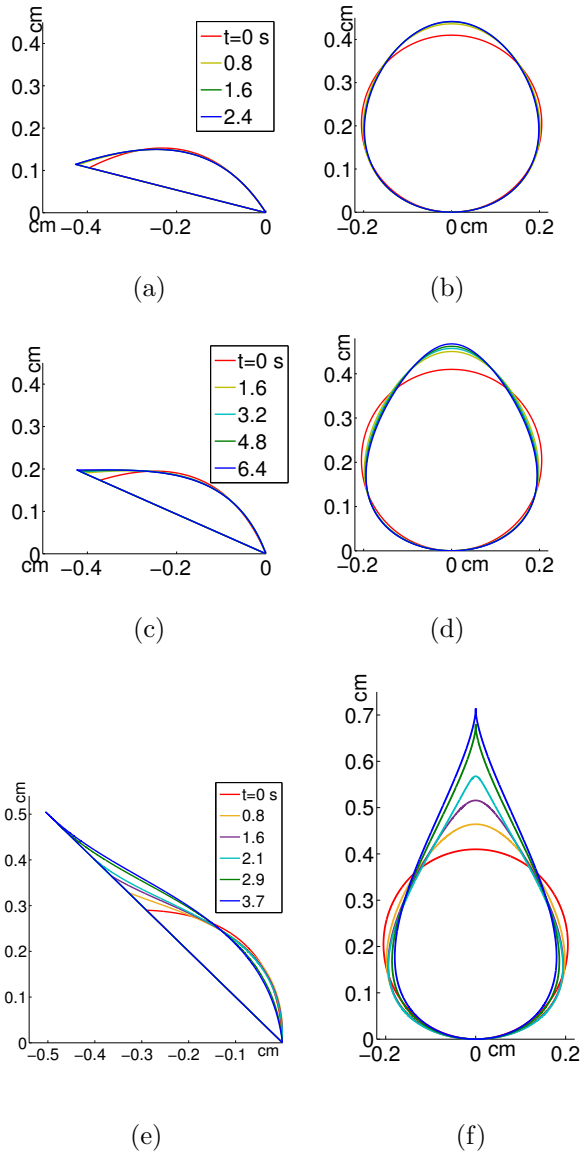

FIG. 6. Shape change of a droplet sliding down on an inclined surface. Left column: side view, right column: top view. (a),(b): $\alpha = 15^{\circ}$, (c),(d): $\alpha = 25^{\circ}$, (e),(f): $\alpha = 45^{\circ}$ The shape becomes steady in (a) and (c), but not in (e).

Fig. 7 shows the relation between the sliding velocity U and the inclination angle α. The sliding velocity U is represented by the capillary number $Ca = \eta U/\gamma$, and the inclination angle is represented by the bond number $Bo_{\alpha} = Bo \sin\alpha = V^{2/3}(\rho g/\gamma)\sin\alpha$. A linear relation is seen between the capillary number and the Bond number. It is seen that the slope of the calculated curve agrees with experimental curve. The agreement is encouraging since no adjustable parameters are used in the calculation. On the other hand, the starting points of the two curves do not agree with each other : the calculated curve starts from the

origin, while the experimental curve is off and below this curve. This is due to the contact angle hysteresis. Experimentally a droplet does not move until the inclination angle exceeds a certain critical angle, while the theory predicts that the droplet starts to move when the substrate is inclined slightly. The discrepancy can be resolved if the effect of hysteresis is included, but such attempt has not been done here.

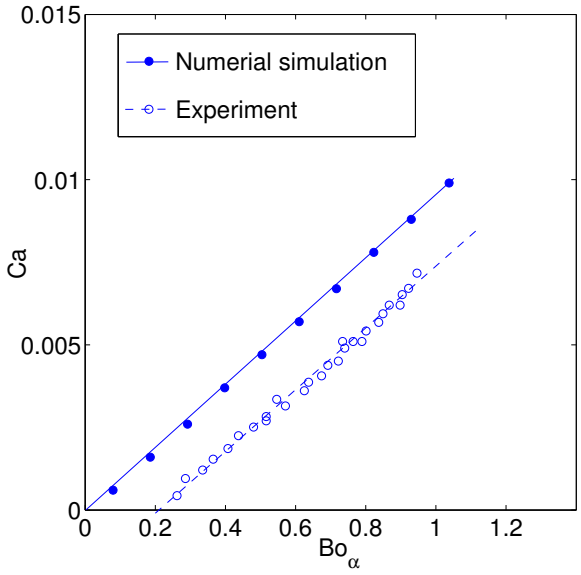

FIG. 7. Capillary-Bond number relations.

Fig. 8 shows the advancing angle and the receding angle plotted against the capillary number. With increasing capillary number, the advancing angle increases and the receding angle decreases. The receding angles in numerical simulation are close to that from experiments, while there is a discrepancy in the advancing angle. This discrepancy can be reduced if the contact angle hysteresis is included, but, again, such refinement has not been attempted. Fig. 9 shows the length(L), the width(W) and the height(H) of the droplet plotted against the capillary number. We see that the height H and the width W agree quite well with the experiments. The agreement is not good for the length L. This is because L is sensitive to the contact angle which shows deviation from experiments as shown in Fig. 8.

Fig. 10 shows a direct comparison for the droplet shape between theory and experiment in Ref. [33]. Here we used the experimental receding angle 42^o(rather than the advancing angle 53^o) for θ_e, and adjusted the cut-off parameters in the numerical calculation. It is seen

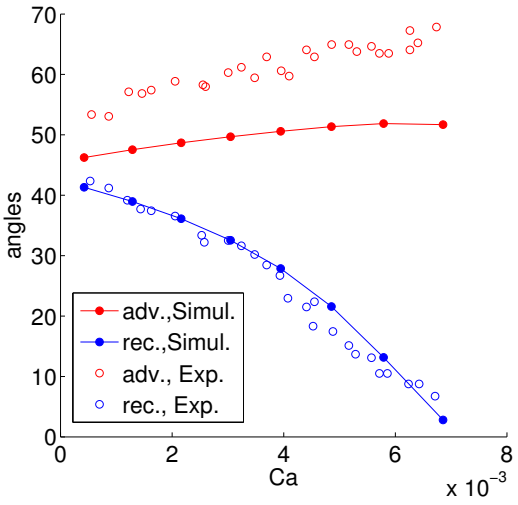

FIG. 8. The advancing angle and receding angle versus the capillary number.

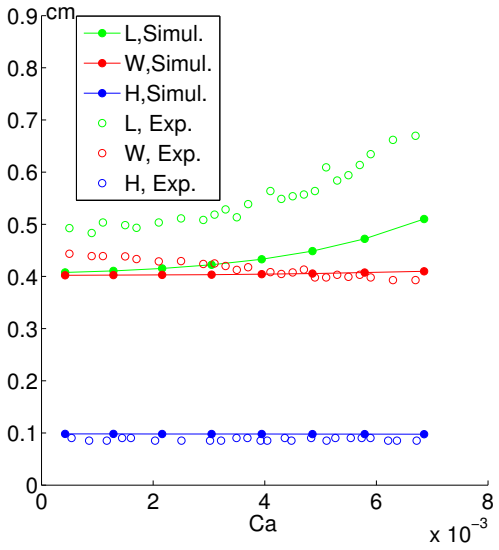

FIG. 9. The length(L), width(W) and height(H) versus the capillary number.

that the numerical results fit the experiments quite well. As the capillary number increases, the shape changes from oval, corner, cusp to rivulet. Once again, we note that, the cusp shape is not a steady state in our numerical simulation, therefore it is compared with the rivulet state in experiments.

Many analyses have been done for the sliding droplet [10–12, 30]. Special attention has been paid on the shape of the rear corner, and its transition to revulets. Our results are qualitatively in agreement with such studies. Clearly, the agreement is not perfect: the

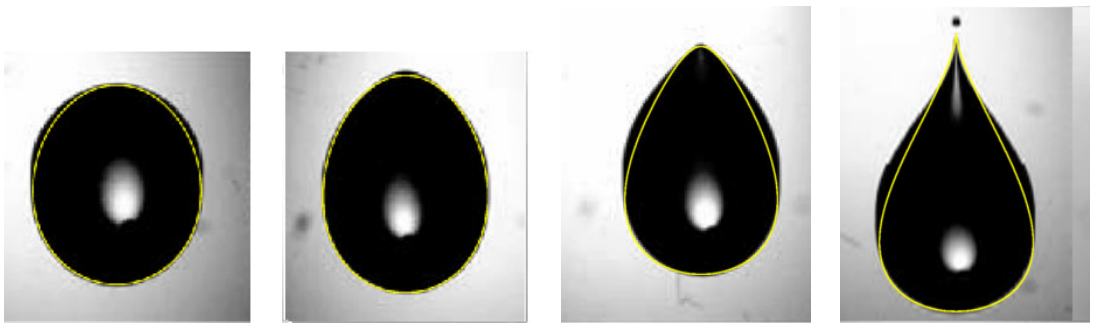

(a) (b) (c) (d)

FIG. 10. Compared with experiments for shape of a droplet at different regimes. (a) oval ($Ca = 2.85 \times 10^{-3}$), (b)corner ($Ca = 4.95 \times 10^{-3}$), (c) corner ($Ca = 5.14 \times 10^{-3}$), (d) cusp(rivulet) ($Ca = 7.19 \times 10^{-3}$).

experimentally observed shape of the rear corner is sharper than that that of the present calculation. On the other hand, it should be stressed that the agreement shown in Fig. 10 has been obtained without using any physical adjustable parameters. All physical quantities used in the calculation are those in the experimental paper except for the cut off parameter ℓ, which we used a typical value reported in literatures[2]. This demonstrates the present simple method has a predictive power useful for practical applications. Better agreement would be obtained if more variational parameters are introduced.

V. DISCUSSION AND CONCLUSION

In this paper, we have shown a variational method to calculate the evolution of liquid droplet sliding on a substrate. We assumed a functional form of the droplet shape, and determined the time evolution of the parameters involved in the functions using the variational principle. This method gives a correct solution if the entire parameter space is searched, but in a limited parameter space (with one or several parameters as in the present examples) it gives approximate solutions. We have demonstrated that, though approximate, the method reproduces characterisitc features of the dynamics of sliding liquid.

The advantage of this method is that it is easy to include various effects. As it has been discussed in ref [19, 34], the variational principle is quite general, and many kinetic equations which have been used to describe the evolution of non-equilibrium system, such as the convective-diffusion equation, Smoluchowskii equation for Brownian motion, Ericksen-Leslie

equation for liquid crystals, gel dynamics equations, are derived from this principle. Therefore the present variational method can be used to solve such wide class of problems. The method has already been applied to a problem of contact line motion with solvent evaporation [22], meniscus rise in elastic capillaries[23]. More examples are now being pursued and will be published in future.

Acknowledgments: X. X. acknowledges the financial support of SRF for ROCS, SEM and NSFC grant(No. 11571354). Y. D. acknowledges the financial support of NSFC grant(No. 11271358). M. D. acknowledges the financial support of the Chinese Central Government in the program of 'Thousand talents' and the NSFC grant (No. 21434001, No.11421110001).

[1] L. Leger and J. F. Joanny. Liquid spreading. *Rep. Prog. Phys.*, 92:431–486, 1992.

[2] Pierre-Gilles De Gennes. Wetting: statics and dynamics. *Reviews of modern physics*, 57(3):827, 1985.

[3] P.-G. De Gennes, F. Brochard-Wyart, and D. Quéré. *Capillarity and wetting phenomena: drops, bubbles, pearls, waves*. Springer Science & Business Media, 2004.

[4] D. Bonn, J. Eggers, J. Indekeu, J. Meunier, and E. Rolley. Wetting and spreading. *Rev. Mod. Phys.*, 81(2):739, 2009.

[5] T. Podgorski, J.-M. Flesselles, and L. Limat. Corners, cusps, and pearls in running drops. *Phys. Rev. lett.*, 87(3):036102, 2001.

[6] E. B. Dussan V. and R. T.-P. Chow. On the ability of drops or bubbles to stick to non-horizontal surfaces of solids. *Journal of Fluid mechanics*, 137:1–29, 1983.

[7] E. B. Dussan V. On the ability of drops or bubbles to stick to non-horizontal surfaces of solids. part 2. small drops or bubbles having contact angles of arbitrary size. *Journal of Fluid Mechanics*, 151:1–20, 1985.

[8] E. B. Dussan V. On the ability of drops to stick to surfaces of solids. part 3. the influences of the motion of the surrounding fluid on dislodging drops. *Journal of Fluid Mechanics*, 174:381–397, 1987.

[9] M. B. Amar, L. J. Cummings, and Y. Pomeau. Transition of a moving contact line from smooth to angular. *Physics of Fluids*, 15(10):2949–2960, 2003.

[10] L. Limat and H. A. Stone. Three-dimensional lubrication model of a contact line corner singularity. *Europhys. Lett.*, 65(3):365, 2004.

[11] J. H. Snoeijer, N. Le Grand-Piteira, L. Limat, H. A. Stone, and J. Eggers. Cornered drops and rivulets. *Physics of Fluids*, 19(4):042104, 2007.

[12] I. Peters, J. H. Snoeijer, A. Daerr, and L. Limat. Coexistence of two singularities in dewetting flows: regularizing the corner tip. *Phys. Rev. Lett.*, 103(11):114501, 2009.

[13] R. Cox. The dynamics of the spreading of liquids on a solid surface. part 1. viscous flow. *J. Fluid Mech.*, 168:169–194, 1986.

[14] Y. D. Shikhmurzaev. *Capillary flows with forming interfaces.* Chapman & Hall CRC, 2008.

[15] Y. Sui, H. Ding, and P. Spelt. Numerical simulations of flows with moving contact lines. *Annual Review of Fluid Mechanics*, 46:97–119, 2014.

[16] M. Maglio and D. Legendre. Numerical simulation of sliding drops on an inclined solid surface. In *Computational and Experimental Fluid Mechanics with Applications to Physics, Engineering and the Environment*, pages 47–69. Springer, 2014.

[17] L. W. Schwartz, D. Roux, and J. J. Cooper-White. On the shapes of droplets that are sliding on a vertical wall. *Physica D: Nonlinear Phenomena*, 209(1):236–244, 2005.

[18] M. Doi. Onsager's variational principle in soft matter. *J. Phys. Cond Matt*, 23:284118 1–8, 2011.

[19] M. Doi. *Soft Matter Physics.* Oxfort University Press, 2013.

[20] M. Doi. Variational principle for the kirkwood theory for the dynamics of polymer solutions and suspensions. *J. Chem. Phys.*, 79, 1983.

[21] M. Doi. Onsager priciple as a tool for approximation. *Chinese Phys. B*, 24:020505, 2015.

[22] X. Man and M. Doi. Ring to mountain transition in deposition pattern of drying droplets. *Physical Review Letters*, 116(6):066101, 2016.

[23] Y. Di, X. Xu, and M. Doi. Theoretical analysis for meniscus rise of a liquid contained between a flexible film and a solid wall. *Europhysics Letters*, 113(3):36001, 2016.

[24] B. R. Duffy and S. K. Wilson. A third-order differential equation arising in thin-film flows and relevant to tanner's law. *Appl. Math. Lett.*, 10(3):63–68, 1997.

[25] J. Eggers. Hydrodynamic theory of forced dewetting. *Physical review letters*, 93(9):094502, 2004.

[26] J. Eggers. Existence of receding and advancing contact lines. *Physics of Fluids*, 17(8):082106,

2005.

[27] L. M. Pismen and J. Eggers. Solvability condition for the moving contact line. *Physical Review E*, 78(5):056304, 2008.

[28] J. H. Snoeijer, G. Delon, M. Fermigier, and B. Andreotti. Avoided critical behavior in dynamically forced wetting. *Physical review letters*, 96(17):174504, 2006.

[29] M. Maleki, E Reyssat., D. Quere, and R. Golestanian. On the landau-levich transition. *Langmuir*, 23(20):10116–10122, 2007.

[30] J. H. Snoeijer, E. Rio, N. Le Grand, and L. Limat. Self-similar flow and contact line geometry at the rear of cornered drops. *Phys. Fluids*, 17(7):072101, 2005.

[31] X.-P. Qian, T. Wang and P. Sheng. Power-law slip profile of the moving contact line in two-phase immiscible flows. *Phys. Rev. lett.*, 63:094501, 2004.

[32] S. Guo, M. Gao, X. Xiong, Y. J. Wang, X.-P. Wang, P. Sheng, and P. Tong. Direct measurement of friction of a fluctuating contact line. *Phys. Rev. Lett.*, 111(2):026101, 2013.

[33] N. Le Grand, A. Daerr, and L. Limat. Shape and motion of drops sliding down an inclined plane. *J. Fluid Mech.*, 541:293–315, 2005.

[34] M. Doi. *Onsager's variational principle in soft matter dynamics, in Non-Equilibrium Soft Matter Physics ed S. Komura and T. Ohta, p 1-35.* World Scientific, 2012.